



Computational Science:
Introduction to Finite-Difference Time-Domain
Metals & Alternative Grids

Lecture Outline

- Incorporating metals into FDTD
- Alternative grids

Incorporating Metals into FDTD

Slide 3

What are Metals?

Metals are materials with very high conductivity σ and usually very negative dielectric constant ϵ_r . The electric field approaches zero inside a metal (i.e. $\vec{E} = 0$).

Increasing Conductivity
↓

Material	Conductivity σ (S/m)
Glass	$\sim 10^{-12}$
Carbon	$\sim 3 \times 10^4$
Mercury	10^6
Lead	3×10^6
Tin	9×10^6
Iron	1.03×10^7
Nickel	1.45×10^7
Aluminum	3.96×10^7
Gold	4.1×10^7
Copper	5.76×10^7
Silver	6.1×10^7

Slide 4

Methods for Incorporating Metals

Easier Implementation
More Accurate Simulation

- Extreme Dielectric Constant
 - Easiest because no modification to the code is necessary, but it does not account for loss.
- Perfect Electric Conductor
 - Requires minimal modification to the code, but does not account for loss.
- σ
 - Requires greater modification to the formulation of the update equations. It can account for loss, but cannot account for frequency dependence.
- Lorentz-Drude Model
 - Requires a much more complicated formulation and implementation, but it can account for loss and frequency dependence.

Method #1: Extreme Dielectric Constant

Recall the update equations for the electric field:

$$\tilde{E}_x|_{t+\Delta t}^{i,j} = \left(\frac{1}{\epsilon_{xx}|^{i,j}} \right) \tilde{D}_x|_{t+\Delta t}^{i,j} \quad \tilde{E}_y|_{t+\Delta t}^{i,j} = \left(\frac{1}{\epsilon_{yy}|^{i,j}} \right) \tilde{D}_y|_{t+\Delta t}^{i,j} \quad \tilde{E}_z|_{t+\Delta t}^{i,j} = \left(\frac{1}{\epsilon_{zz}|^{i,j}} \right) \tilde{D}_z|_{t+\Delta t}^{i,j}$$

In metals, the electric field approaches zero. We can force this to happen by choosing dielectric constants that are very large (i.e. 10^3 or higher).

$$\text{As } \epsilon_{xx}|^{i,j} \rightarrow \infty, \quad \tilde{E}_x|_{t+\Delta t}^{i,j} \rightarrow 0$$

$$\text{As } \epsilon_{yy}|^{i,j} \rightarrow \infty, \quad \tilde{E}_y|_{t+\Delta t}^{i,j} \rightarrow 0$$

$$\text{As } \epsilon_{zz}|^{i,j} \rightarrow \infty, \quad \tilde{E}_z|_{t+\Delta t}^{i,j} \rightarrow 0$$

Method #2: Perfect Electric Conductor

Recall the update equations for the electric fields:

$$\tilde{E}_x|_{t+\Delta t}^{i,j} = (m_{Ex1}|_{t+\Delta t}^{i,j}) \tilde{D}_x|_{t+\Delta t}^{i,j} \quad \tilde{E}_y|_{t+\Delta t}^{i,j} = (m_{Ey1}|_{t+\Delta t}^{i,j}) \tilde{D}_y|_{t+\Delta t}^{i,j} \quad \tilde{E}_z|_{t+\Delta t}^{i,j} = (m_{Ez1}|_{t+\Delta t}^{i,j}) \tilde{D}_z|_{t+\Delta t}^{i,j}$$

The fields can be forced to zero by setting the update coefficients to 0 everywhere there is a metal and 1 everywhere that there is not.

Define the placement of metals using three arrays:

$$\text{PEC}_x|_{t+\Delta t}^{i,j,k} \quad \text{PEC}_y|_{t+\Delta t}^{i,j,k} \quad \text{PEC}_z|_{t+\Delta t}^{i,j,k}$$

Modify the update coefficients as follows:

$$m_{Ex1}|_{t+\Delta t}^{i,j,k} = (\text{PEC}_x|_{t+\Delta t}^{i,j,k}) (m_{Ex1}|_{t+\Delta t}^{i,j,k})$$

$$m_{Ey1}|_{t+\Delta t}^{i,j,k} = (\text{PEC}_y|_{t+\Delta t}^{i,j,k}) (m_{Ey1}|_{t+\Delta t}^{i,j,k})$$

$$m_{Ez1}|_{t+\Delta t}^{i,j,k} = (\text{PEC}_z|_{t+\Delta t}^{i,j,k}) (m_{Ez1}|_{t+\Delta t}^{i,j,k})$$

Method #3: Conductivity σ

Recall from previous lectures that material conductivity can be incorporated into Maxwell's equations as follows:

$$\nabla \times \vec{E} = -\mu \frac{\partial \vec{H}}{\partial t} \quad \nabla \times \vec{H} = \sigma \vec{E} + \varepsilon \frac{\partial \vec{E}}{\partial t}$$

Metals can be accounted for by retaining this conductivity term, deriving new update equations, and revising the FDTD algorithm.

Note, three new materials arrays will need to be defined:

$$\sigma_{xx}, \sigma_{yy}, \sigma_{zz}$$

Method #4: Lorentz-Drude Model

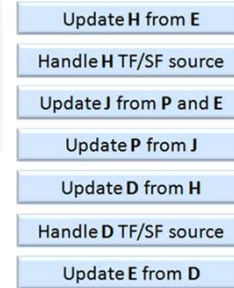
Recall from previous lectures that the constitutive relation can be written as

$$\vec{D}(\omega) = \epsilon_0 \epsilon_\infty \vec{E}(\omega) + \vec{P}(\omega) \quad \vec{P}(\omega) = \omega_p^2 \vec{E}(\omega) \sum_{m=1}^M \frac{f_m}{\omega_{0,m}^2 - \omega^2 + j\omega\Gamma_m}$$

This can be implemented in the time-domain as follows

$$\frac{\partial}{\partial t} \vec{J}_m(t) + \Gamma_m \vec{J}_m(t) + \omega_{0,m}^2 \vec{P}_m(t) = f_m \omega_p^2 \vec{E}(t)$$

$$\vec{J}_m(t) = \frac{\partial}{\partial t} \vec{P}_m(t)$$



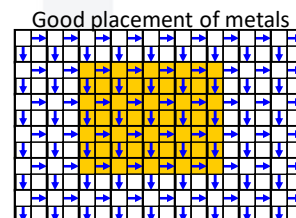
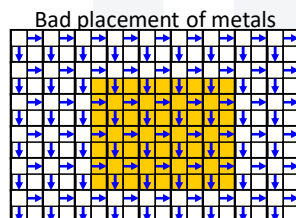
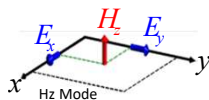
Placing Metals on a 2D Grid

Ez Mode

For the E_z mode, the electric field is always tangential to metal interfaces and few problems arise when modeling metallic structures.

H_z Mode

For the H_z mode, the electric field can be polarized perpendicular to metal interfaces. This is problematic and it is best to place metals with the outermost fields being tangential to the interfaces.

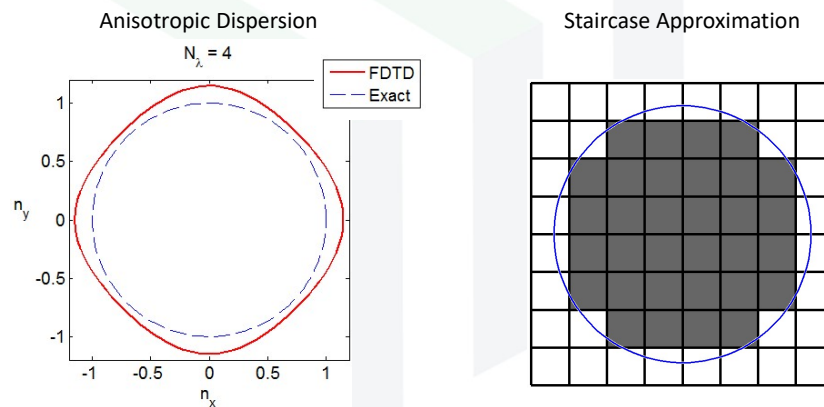


Alternative Grids

Slide 11

Drawbacks of Uniform Grids

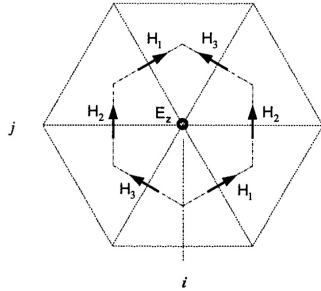
Uniform grids are the easiest to implement, but do not conform well to arbitrary structures and exhibit high anisotropic dispersion.



Slide 12

Hexagonal Grids

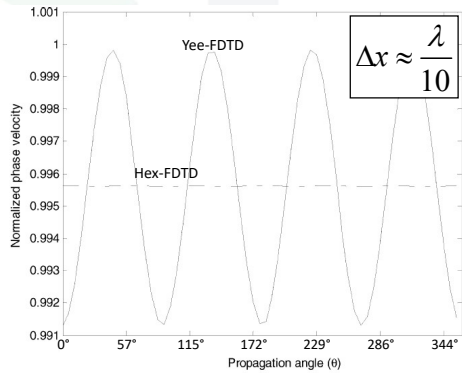
Hexagonal grids are good for minimizing anisotropic dispersion suffered on Cartesian grids. This is very useful when extracting phase information.



(b) Staggered, uncollocated grid and its associated dual grid

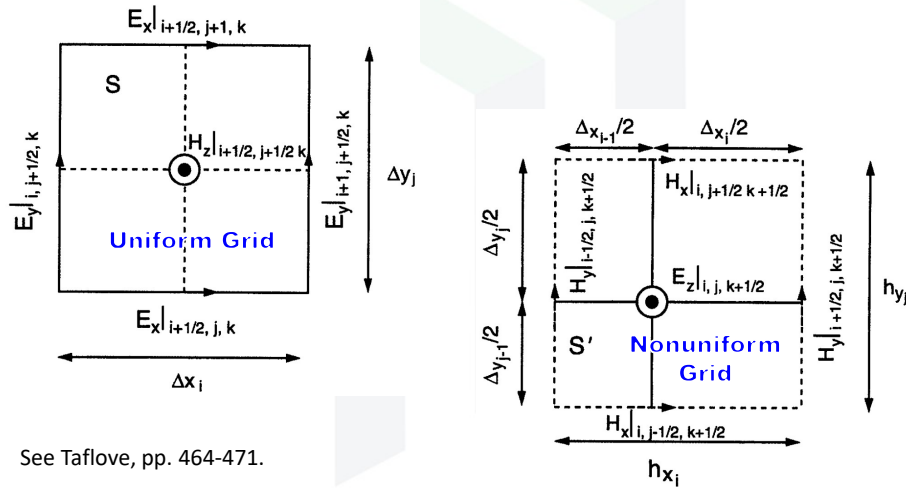
See Text, pp. 101-103.

Phase Velocity as a Function of Propagation Angle



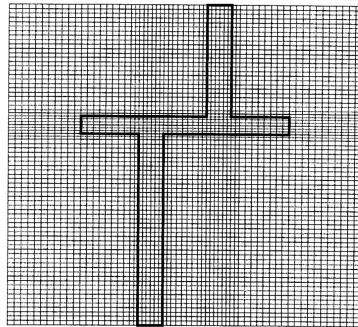
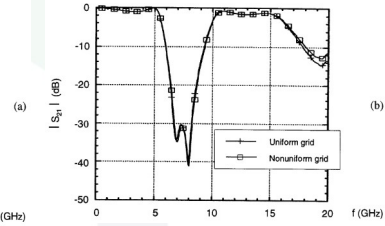
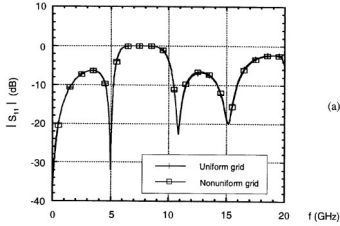
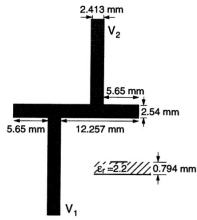
Nonuniform Orthogonal Grids (1 of 2)

Nonuniform orthogonal grids are still relatively simple to implement and provide some ability to refine the grid at localized regions.



See Taflove, pp. 464-471.

Nonuniform Orthogonal Grids (2 of 2)



Uniform Grid Simulation

- 80×110×16 cells
- 140,800 cells

Nonuniform Grid Simulation

- 64×76×16 cells
- 77,824 cells

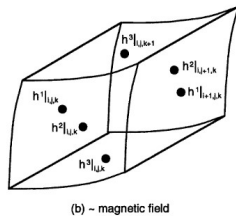
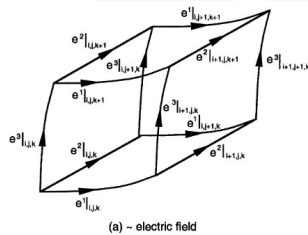
Conclusion: Roughly 50% memory and time savings.



Slide 15

Curvilinear Coordinates

Maxwell's equations can be transformed from curvilinear coordinates to Cartesian coordinates to conform to curved boundaries of a device.



See Text, pp. 484-492.

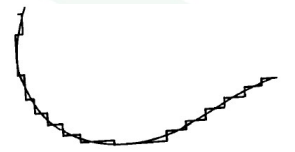


Fig. 2. Staircasing approximation to a curved boundary.



Fig. 3. Cell deformation in vicinity of a curved boundary.

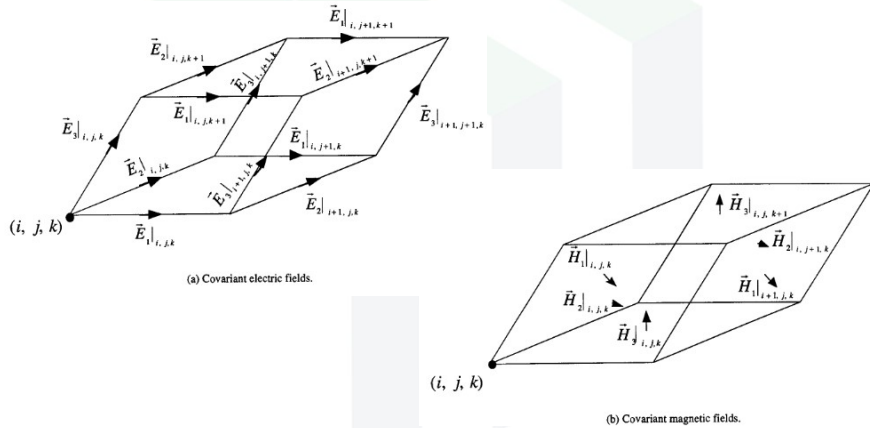
M. Fusco, "FDTD Algorithm in Curvilinear Coordinates," IEEE Trans. Ant. and Prop., vol. 38, no. 1, pp. 76-89, 1990.



Slide 16

Structured Nonorthogonal Grids

This is a particularly powerful approach for simulating periodic structures with oblique symmetries.



M. Fusco, "FDTD Algorithm in Curvilinear Coordinates," IEEE Trans. Ant. and Prop., vol. 38, no. 1, pp. 76-89, 1990.



Slide 17

Irregular Nonorthogonal Unstructured Grids

Unstructured grids are more tedious to implement, but can conform to highly complex shapes while maintaining good cell aspect ratios and global uniformity.

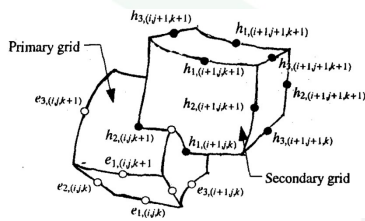


Fig. 2. Sparse and dense nonorthogonal grids for the cylindrical cavity.

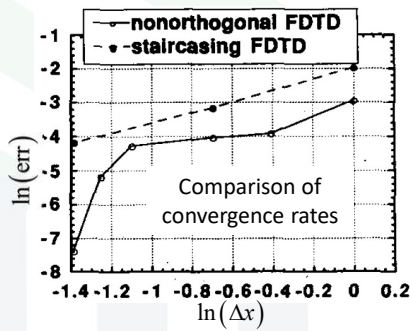


Fig. 3. Sparse and dense staircase grids for the cylindrical cavity.

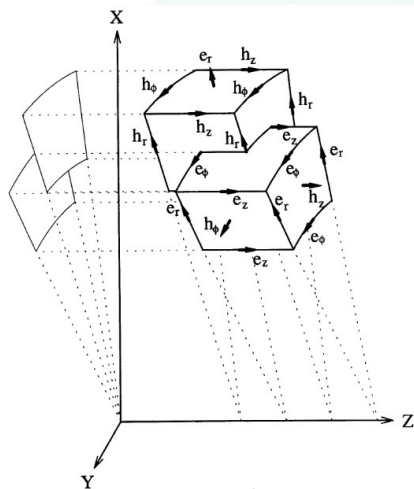


P. Harms, J. Lee, R. Mittra, "A Study of the Nonorthogonal FDTD Method Versus the Conventional FDTD Technique for Computing Resonant Frequencies of Cylindrical Cavities," IEEE Trans. Microwave Theory and Techniq., vol. 40, no. 4, pp. 741-746 , 1992.

Slide 18

Bodies of Revolution (Cylindrical Symmetry)

Three-dimensional devices with cylindrical symmetry can be very efficiently modeled using cylindrical coordinates.



Devices with cylindrical symmetry have fields that are periodic around their axis. Therefore, the fields can be expanded into a Fourier series in ϕ .

$$\vec{E}(\rho, \theta, \phi) = \sum_{m=0}^{\infty} \vec{e}_{\text{even}}(\rho, \theta) \cdot \cos(m\phi) + \vec{e}_{\text{odd}}(\rho, \theta) \cdot \sin(m\phi)$$

$$\vec{H}(\rho, \theta, \phi) = \sum_{m=0}^{\infty} \vec{h}_{\text{even}}(\rho, \theta) \cdot \cos(m\phi) + \vec{h}_{\text{odd}}(\rho, \theta) \cdot \sin(m\phi)$$

Due to a singularity at $r=0$, update equations for fields on the z axis are derived differently.

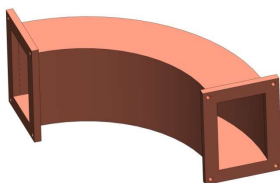
See Text, Chapter 12



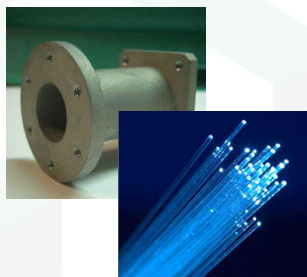
Slide 19

Some Devices with Cylindrical Symmetry

Bent Waveguides



Cylindrical Waveguides



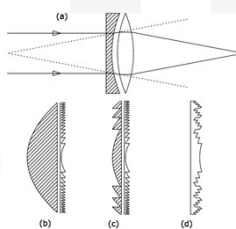
Dipole Antennas



Conical Horn Antenna



Diffractive Lenses



Focusing Antennas



Slide 20